

## Edge-spin-derived magnetism in few-layer MoS<sub>2</sub> nanomeshes

G. Kondo, N. Yokoyama, S. Yamada, Y. Hashimoto, C. Ohata, S. Katsumoto, and J. Haruyama

Citation: *AIP Advances* **7**, 125019 (2017);

View online: <https://doi.org/10.1063/1.4989477>

View Table of Contents: <http://aip.scitation.org/toc/adv/7/12>

Published by the [American Institute of Physics](#)

---

---

# HAVE YOU HEARD?

Employers hiring scientists and  
engineers trust

**PHYSICS TODAY | JOBS**

[www.physicstoday.org/jobs](http://www.physicstoday.org/jobs)



## Edge-spin-derived magnetism in few-layer MoS<sub>2</sub> nanomeshes

G. Kondo,<sup>1</sup> N. Yokoyama,<sup>1</sup> S. Yamada,<sup>1</sup> Y. Hashimoto,<sup>2</sup>  
C. Ohata,<sup>1</sup> S. Katsumoto,<sup>2</sup> and J. Haruyama<sup>1,2,a</sup>

<sup>1</sup>Faculty of Science and Engineering, Aoyama Gakuin University, 5-10-1 Fuchinobe, Sagamihara, Kanagawa 252-5258, Japan

<sup>2</sup>Institute for Solid State Physics, The University of Tokyo, 5-1-5 Kashiwanoha, Kashiwa, Chiba 277-8581, Japan

(Received 28 April 2017; accepted 6 December 2017; published online 21 December 2017)

Magnetism arising from edge spins is highly interesting, particularly in 2D atomically thin materials in which the influence of edges becomes more significant. Among such materials, molybdenum disulfide (MoS<sub>2</sub>; one of the transition metal dichalcogenide (TMD) family) is attracting significant attention. The causes for magnetism observed in the TMD family, including in MoS<sub>2</sub>, have been discussed by considering various aspects, such as pure zigzag atomic-structure edges, grain boundaries, and vacancies. Here, we report the observation of ferromagnetism (FM) in few-layer MoS<sub>2</sub> nanomeshes (NMs; honeycomb-like array of hexagonal nanopores with low-contamination and low-defect pore edges), which have been created by a specific non-lithographic method. We confirm robust FM arising from pore edges in oxygen(O)-terminated MoS<sub>2</sub>-NMs at room temperature, while it disappears in hydrogen(H)-terminated samples. The observed high-sensitivity of FM to NM structures and critical annealing temperatures suggest a possibility that the Mo-atom dangling bond in pore edge is a dominant factor for the FM. © 2017 Author(s). All article content, except where otherwise noted, is licensed under a Creative Commons Attribution (CC BY) license (<http://creativecommons.org/licenses/by/4.0/>). <https://doi.org/10.1063/1.4989477>

Edge-spin-derived magnetism in 2D atomically thin materials is a key to fabricate flexible magnetic and spintronic devices without using rare-earth magnetic elements. It was theoretically well known that high electronic density of states (the so-called edge states) originating from the flat energy band of the zigzag-type atomic structure of graphene nanoribbons (GNRs) leads to the appearance of flat-band FM. This has been experimentally confirmed in H-terminated zigzag-edged GNRs and also in our H-terminated graphene nanomeshes (H-GNMs).<sup>1,2</sup> Because the GNMs were fabricated using a specific non-lithographic method (i.e., low-power etching of graphene using a nanoporous alumina template mask), the pore edges controlled by critical-temperature annealing were obtained with the small amount of disorder and contamination, which resulted in a zigzag atomic structure of pore-edges through edge-atomic reconstruction as explained in later. Because a NM structure has a large ensemble of GNRs (i.e., corresponding to the interpore narrow regions with 10–20 nm width) and zigzag pore edges, small magnetic signals arising from the pore edge spins of a GNM could be effectively detected even at room temperature.

We also adopted this NM structure to few-layer black phosphorus (BP; a 2D semiconductor with a substantial energy band gap intermediating between the zero-gap graphene and the large band-gap of TMD family),<sup>3</sup> and to few-layer hexagonal boron-nitride (hBN; an insulator (with a wide band gap of 5.92 eV) composed of a hexagonal network with an equal number of alternating B and N atoms in *sp*<sup>2</sup> hybridization that are bonded covalently).<sup>4</sup> We revealed that the O-terminated few-layer zigzag BP-NMs produce evident room-temperature FM with a magnitude approximately 100 times/area

<sup>a</sup>Email: [J-haru@ee.aoyama.ac.jp](mailto:J-haru@ee.aoyama.ac.jp)

larger than that reported for the H-GNMs at room temperature.<sup>3</sup> The O-terminated zigzag-hBN-NM also exhibited similar room-temperature FM with a much smaller amplitude.<sup>4</sup> On the other hand, in H-terminated BP-NM and hBN-NM, these FMs disappeared. These behaviors were in contrast to the case of abovementioned GNM, which demonstrated FM in H-terminated samples but not in O-terminated samples. Because both BP-NM and hBN-NM have no flat energy band, the observed magnetism has been understood from different mechanisms; i.e., ferromagnetic spin coupling in the edge P=O bond in BP-NMs and spin splitting in  $p_x$  and  $p_z$  orbitals of the edge O-N bond in hBN-NM.

Here, atom-thin MoS<sub>2</sub> is attracting significant attention because of its direct bandgap of 1.5–1.8 eV in the 2H semiconducting phase.<sup>5</sup> We reported an atomically thin MoS<sub>2</sub> lateral Schottky junction created only by electron beam irradiation that caused (2H-semiconductor)-to-(1T-metal) phase transition,<sup>6</sup> and its photoresponse.<sup>7</sup> Various phenomena and applications of atomically thin TMD family, and also their van der Waals (vdW) heterostructure with other 2D atomically thin layers have been reported. Magnetism derived from edge spins has been also reported in TMD family (e.g., MoS<sub>2</sub>, MoSe<sub>2</sub>, WS<sub>2</sub>).<sup>8–16</sup> The causes for magnetism have been discussed by considering various aspects, such as zigzag edges,<sup>8–10</sup> grain boundaries,<sup>11</sup> vacancies,<sup>12</sup> ion irradiation,<sup>17</sup> and Mo-doping.<sup>18</sup> However, no consensus has been reached regarding these. Each layer of TMD family typically has a thickness of 6–7 Å, which consists of a hexagonally packed layer of metal atoms sandwiched between two layers of chalcogen atoms (Fig. 1(a)(b)).<sup>5</sup> Therefore, two different kinds of dangling bonds at zigzag edges exist over the two atom layers within the AB stacking structure; e.g., one zigzag edge of a NR has a Mo dangling bond (right red circle of Fig. 1(a)), while the other has a S dangling bond (left blue circle of Fig. 1(a)). In this sense, the termination of these different edge dangling bonds by foreign atoms is analogous to the case of the edge dangling bonds of hBN-NR, in which only the edge O-N bond yielded FM, as mentioned above. Thus, it is interesting to clarify which dangling bonds in the zigzag edges of MoS<sub>2</sub> are a dominant factor for FM.

In this work, flakes of few-layer MoS<sub>2</sub> are mechanically exfoliated on SiO<sub>2</sub>/Si substrate from bulk MoS<sub>2</sub> (Smart Element Co.) in a glove box using the (non-magnetic) Scotch tape method and confirmed using optical and atomic force microscopies (Fig. 2(a)(b)) and Raman spectroscopy (Fig. 2(c)). Both the in-plane E<sub>12g</sub> (382 cm<sup>-1</sup>) and the out-of-plane A<sub>1g</sub> (487 cm<sup>-1</sup>) vibration modes are confirmed for bulk sample in Fig. 2(c). A thickness of ~3 nm is also confirmed in Fig. 2(b). These suggest that the bulk MoS<sub>2</sub> flake is at least five-layer thick. Similar flakes are collected for magnetization measurement so as to satisfy the total area of ~1cm<sup>2</sup>. Following the abovementioned non-lithographic method (supplementary material),<sup>1–4</sup> few-layer MoS<sub>2</sub>-NMs are fabricated and confirmed by field-emission SEM (FESEM) (Fig. 2(d)) and atomic force microscopy. The absence of magnetic impurities (e.g., Ni, Co, and Fe) is also confirmed by X-ray Photoelectron Spectroscopy (Fig. 2(e)). Interpore narrow regions (e.g.,  $w \sim 10\text{--}20$  nm width) correspond to MoS<sub>2</sub>-NRs as well as the cases for GNMs, few-layer BP-NMs, and few-layer hBN-NMs, as mentioned above.

All the NM samples are annealed at high temperatures for 30 min under high vacuum. Raman spectrum are shown in Fig. 2(c). The peaks become broad and full width of half maximum (FWHM) increases from bulk (e.g. A<sub>1g</sub> ~7 cm<sup>-1</sup>) to pore formation without annealing (A<sub>1g</sub> ~20 cm<sup>-1</sup>). After

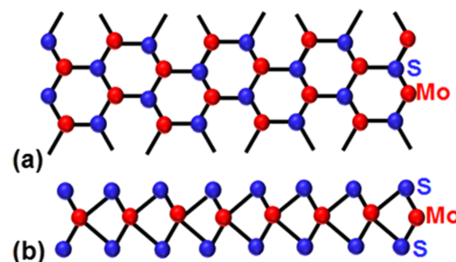


FIG. 1. Schematic (a) top and (b) cross-sectional views of MoS<sub>2</sub> atomic structure: (a) shows a pucker honeycomb lattice over two layers, including zigzag edges with Mo and S dangling bonds on right and left edges of different layers (shown in (b)), respectively.

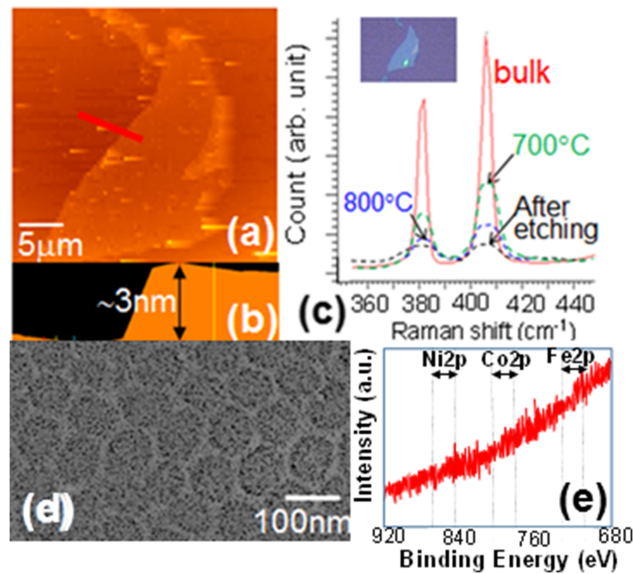


FIG. 2. (a, b) Typical atomic force microscope images of a mechanically exfoliated MoS<sub>2</sub> flake: (a) top and (b) cross sectional views. (b) is obtained along the red line shown in (a). (c) Typical Raman spectrum of the bulk flake (red curve) and nanomesh right after pore formation without annealing (black-dot curve) and right after 700 °C- and 800 °C-annealing (green and blue dot curves, respectively). Inset: Optical microscope image of a measured MoS<sub>2</sub> flake. White spot means the part irradiated by laser beam. (d) FESEM top-view images of a MoS<sub>2</sub>-NM formed on the sample in (a) with difference observation scales. The mean pore diameter ( $\Phi$ ) and interpore distance ( $w$ ) are  $\sim 80$  nm and  $\sim 10$  nm, respectively. (e) Typical XPS spectra of a ferromagnetic MoS<sub>2</sub>-NM (Fig. 3(a)-sample) for binding energy of orbitals of Ni2p, Co2p, and Fe2p. Diameter of the irradiated X ray is  $\sim 100$   $\mu$ m. The upper limit for impurity detection of the XPS is 0.05 at%.

the 700 °C annealing, the peak becomes sharp again and FWHM decreases to  $A_{1g} \sim 12$   $\text{cm}^{-1}$ , while it becomes broader and FWHM increases to  $A_{1g} \sim 15$   $\text{cm}^{-1}$  after the 800 °C annealing. As an interpretation, these results mean that the quality of sample degrades by forming NM structure by Ar ion etching, while it recovers by the 700 °C annealing. On the other hand, higher T annealing (i.e., the 800 °C annealing) reduces the sample quality again. Another interpretation should be associated with one dimensional (1D) structure (i.e., NR) of the interpore region of NM, because, in the case of graphene NM, larger D-peak height corresponded to the appearance of arm chair edge in 1D GNR (i.e., the interpore region of graphene NM). Three peak heights do not reach to those of bulk sample because the area of remained interpore regions in NM is very small. Moreover, it suggest absence of defects because there are no peaks other than  $E_{12g}$  and  $A_{1g}$  peaks, unlike reported by Ref. 19. After the annealing, the NMs are exposed to air for the O-termination of pore edges, while they are annealed at a high temperature in a H atmosphere for 30 min for the H-termination.

Figure 3(a) shows a typical measurement result of the magnetization curves of the O-terminated few-layer MoS<sub>2</sub>-NM (O-MoS<sub>2</sub>-NM) annealed at 700 °C (measured by using the superconducting quantum interference device of Quantum Design). Ferromagnetic hysteresis loops are clearly observed with saturation and residual magnetization values  $\sim 6 \times 10^{-4}$   $\text{emu}/150\mu\text{m}^2$  and coercivity  $\sim 100$  Oe. These saturation and residual magnetization values are a few-times larger than those of O-terminated hBN-NMs with a similar area, while smaller than those of O-terminated BP-NMs. The coercivity is almost the same as that of O-hBN-NMs. The hysteresis loop at  $T = 3.5$  K remains almost unchanged even with increasing temperature up to  $T = 300$  K. Because the bulk few-layer MoS<sub>2</sub> flakes without pores exhibit almost no FMs (Fig. 3(c); [supplementary material](#)), the observed robust FM originates solely from the formation of O-terminated nanopore edges in NMs. On the other hand, the FM disappears in H-terminated samples as shown in Fig. 3(b). These are similar to the results observed for BP-NMs and hBN-NMs. This suggests that the ferromagnetic spin alignment between the edge O atom and Mo (or S) dangling bonds in zigzag pore edges is strongly associated with the observed FM.

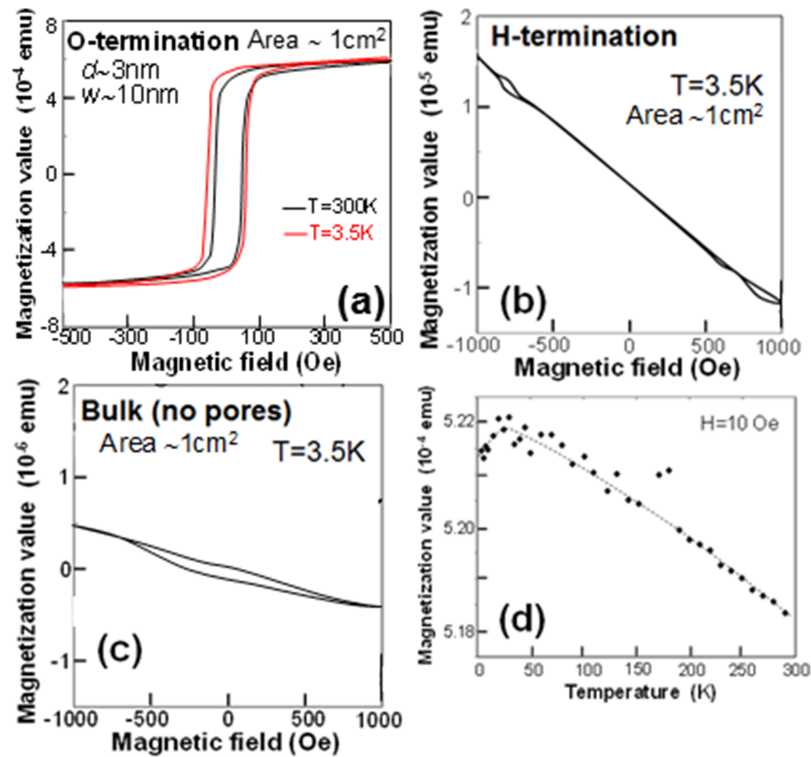


FIG. 3. Typical measurement results of the magnetization curves of the (a) O-terminated and (b) H-terminated few-layer MoS<sub>2</sub>-NM, and (c) bulk MoS<sub>2</sub> flake without pores. Background magnetism of (c) is subtracted in (a). All samples have been annealed at 700 °C under high vacuum. (d) Temperature dependence of the magnetization field of the sample in (a) at a fixed  $H = 10$  Oe. The dotted curve is a guide to the eye.

Figure 3(d) shows the temperature dependence of magnetization of the sample shown in Fig. 3(a) at  $H = 10$  Oe. Magnetization monotonically decreases with increasing temperature up to 300 K, which is the upper limit temperature of our SQUID. Hence, the Currie temperature of this sample is estimated to be above 300 K. It is also interesting to note that the magnetization value slightly increases below 10 K with decreasing temperature.

Figures 4(a) and 4(b) show the saturation magnetization values ( $M_s$ ) of O-terminated samples annealed at 700 °C as a function of the interpore distance ( $w$ ) and sample thickness ( $d$ ).  $M_s$  monotonically increases with increasing  $w$  and  $d$ . Figure 4(c) exhibits the magnetization curves for two different annealing temperatures. The FM observed in samples annealed at 700 °C almost disappears in the samples annealed at above 800 °C. The inset of Fig. 4(c) exhibits  $M_s$  as a function of the annealing temperature. It implies that the annealing temperature has an optimum value to yield a large  $M_s$  (i.e., 700 °C). We have defined  $T_{an}$  as the highest annealing temperature at which the NM structure is maintained even after annealing. The NM structure disappears due to pore-edge atomic reconstruction by annealing at temperatures slightly above  $T_{an}$  (~20 °C), because the interpore regions are NRs with widths as low as 10–20 nm (supplementary material). The amplitudes of FMs observed in H-terminated GNMs<sup>1</sup> and O-terminated BP-NMs<sup>3</sup> actually showed the largest values, when the samples were annealed at this  $T_{an}$ . In contrast, the present MoS<sub>2</sub>-NM structure disappears after annealing at ~820 °C and thus  $T_{an}$  should be ~800 °C, whereas the largest  $M_s$  is obtained for annealing at 700 °C in Fig. 4(c). This is in contrast to the cases for GNMs and BP-NMs, while it is qualitatively similar to those of hBN-NMs, in which  $T_{an}$  was ~600 °C but the annealing temperature for the largest  $M_s$  was 500 °C.<sup>4</sup>

As mentioned above, magnetism in atomically thin MoS<sub>2</sub> layer has been discussed by considering various aspects, such as pure zigzag edges,<sup>8</sup> grain boundaries (e.g., composed of pentagon-heptagon pairs),<sup>11</sup> and vacancies (e.g., arising from 2H/1T-phase combination,<sup>12</sup> with impurity-doping). However, this does not correspond to the present case, because the samples without annealing, which

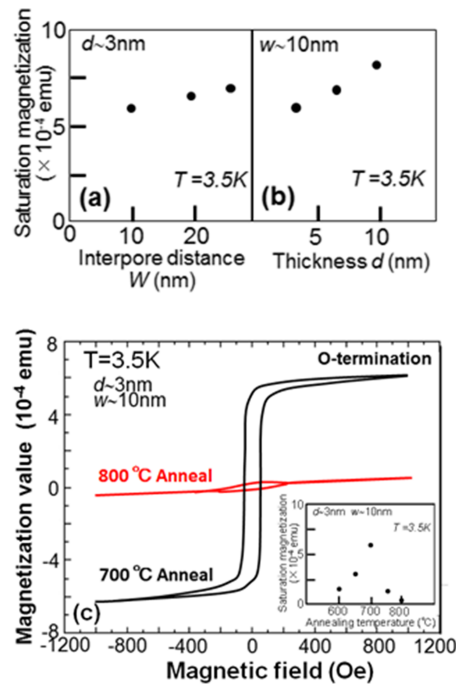


FIG. 4. Saturation magnetization values ( $M_s$ ) of O-terminated samples annealed at 700 °C as a function of (a) inter-pore distance ( $w$ ) and (b) sample thickness ( $d$ ). (c) Magnetization curves of the O-terminated few-layer MoS<sub>2</sub>-NM annealed at two different temperatures, including that shown in Fig. 3(a). Inset of (c):  $M_s$  values as a function of annealing temperature.

should have the largest amount of as-grown defects or boundaries, did not show FM. Moreover, if irregular boundaries and defects are the cause of FM, the exact structure dependence (Figs. 4(a) and (b)) should not appear. Raman spectrum (Fig. 2(c)) support absence of such defects in NMs after the 700 °C annealing. Therefore, we interpret that the contribution of the possible pure zigzag pore edges might be dominant for the present FMs.

We discuss about the relationship between the observed FM and the zigzag edges at pores. Li *et al.*<sup>8</sup> calculated that pure zigzag-edged MoS<sub>2</sub> NRs without termination by foreign atoms provided a stable ferromagnetic ground state with an energy difference  $\Delta E$  between their spin-unpolarized and spin-polarized total energies. Both  $\Delta E$  and the total magnetic moment increased with increasing NR width and thickness (i.e., number of layers). For example, the largest-width MoS<sub>2</sub> NR had the highest  $\Delta E$  (57.30 meV) and a total magnetic moment as large as  $0.879 \mu_B$ . Moreover, the unpaired spin mainly concentrated on the edge Mo and S atoms, while the inner Mo atoms less contributed to the unpaired spin. Densities of the unpaired spins in Mo atom dangling bonds in zigzag edges (e.g., right red circle of Fig. 1(a)) were much larger than those at S atoms (e.g., left blue circle of Fig. 1(a)). On the other hand, the H-terminated zigzag MoS<sub>2</sub> NRs (the edge S and Mo atoms are saturated with one and two H atoms, respectively) showed weaker magnetism.

These theories qualitatively and partially agree with our observation as follows. As mentioned above, inter-pore regions correspond to NRs in our NM structure and the observed FM slightly increases with increasing  $W$  (i.e., NR width; Fig. 4(a)) and  $d$  (Fig. 4(b)). Moreover, the FM amplitude decreases in H-terminated MoS<sub>2</sub>-NMs (Fig. 3(b)).

Because the observed magnetism is for collected NMs, we can estimate the magnetic moment per pore edge dangling bond with O termination  $\sim 1.3 \mu_B$  (supplementary material). This estimation value is larger than that of the abovementioned calculation result  $0.879 \mu_B$ , because this estimation includes magnetization value of O atom terminating the edge dangling bond. Indeed, for few-layer BP-NM, we calculated large magnetic moment of  $0.55 \mu_B$  for P atom at edge dangling bond and that of  $0.4 \mu_B$  for O atom terminating it. Ferromagnetic spin coupling in the edge P=O bond in BP-NMs was the cause for the ferromagnetism in the case. It should correspond to the edge M=O bond in the present case as discussed later.

Here,  $T_{\text{an}}$  ( $\sim 800$  °C) and the annealing temperature to obtain the largest  $M_s$  (700 °C) are different, as mentioned for Fig. 4(c). This can be interpreted that the annealing temperature to form the most stable pore edges with Mo dangling bonds is 700 °C, which results in the densities of the unpaired spins at Mo dangling bonds and the observed largest  $M_s$  (Ref. 8). As discussed above, annealing at  $T_{\text{an}}$  results in the formation of assumed zigzag pore edges through edge atomic reconstruction in our NM structure. This is because NMs disappear by annealing over  $T_{\text{an}}$  and zigzag edge is the most stable from the chemical and thermal viewpoints after the edge atomic reconstruction caused by annealing at  $T_{\text{an}}$ . In both GNM and BP-NM, this  $T_{\text{an}}$  and annealing temperature to obtain the largest FM are the same, because these NMs consist of a single-kind atom (i.e., carbon and black phosphorus, respectively).

In contrast, few-layer hBN-NMs exhibited a relationship with the annealing temperature similar to that of the present few-layer MoS<sub>2</sub>-NMs. As a common structure, MoS<sub>2</sub> and hBN consist of two-different kind atoms (i.e., Mo and S, and B and N, respectively). Consequently, in hBN-NM, there were two different kinds of edge dangling bonds (i.e., B and N atoms) and only the edge O-N bond theoretically yielded FM due to the evident spin splitting in its  $p_x$  and  $p_z$  orbitals.<sup>4</sup> Thus, we interpreted that the pore edges of hBN-NM became N dangling-bond rich after annealing at the temperature for the largest  $M_s$  ( $\sim 500$  °C), while the pore edges became disorder-dominant with non-zigzag by after annealing at  $T_c$  ( $\sim 600$  °C) and FM disappeared. This is because N dangling bonds had a binding energy larger than that for B dangling bonds and they could become sufficiently stable after annealing at temperature  $\sim 500$  °C through the edge-atomic reconstruction. After annealing at much higher temperature ( $\sim 600$  °C), even these pore edges with N dangling bond were destroyed, while inter-pore bulk-parts of hBN-NMs still remained due to the strong B-N bonds.

This mechanism should be analogous to the present MoS<sub>2</sub>-NMs. As calculated by Li *et al.*,<sup>8</sup> edge Mo dangling bonds exhibit an unpaired spin density higher than that of S dangling bonds. Hence, it is speculated that the pore edges of MoS<sub>2</sub>-NM become Mo dangling bonds rich after the annealing at temperature for the largest  $M_s$  ( $\sim 700$  °C), while the pore edges become disorder-dominant with non-zigzag after annealing at  $T_c$  ( $\sim 800$  °C) but keeping the inter-pore bulk-parts of NM structure and FM disappears. This is also because Mo dangling bonds have a binding energy ( $\sim 232$  eV for 3d<sub>3/2</sub> and  $\sim 229$  eV for 3d<sub>5/2</sub>) larger than that of S dangling bonds ( $\sim 164$  eV for 2p<sub>1/2</sub> and  $\sim 162$  eV for 2p<sub>3/2</sub>).<sup>6</sup> In the O-terminated hBN-NMs, the evident spin splitting in  $p_x$  and  $p_z$  orbitals of the edge O-N bond led to the FM. In the present case, Mo dangling bonds have unsaturated bonds in core 3d<sub>3/2</sub> and 3d<sub>5/2</sub> orbitals at least. O-termination of these unsaturated bonds should lead to the significant spin splitting and the observed FM. With this viewpoint, the theoretical confirmation of the mechanism of ferromagnetic spin coupling at the edge O-Mo bonds is indispensable.

The ferromagnetic spin coupling at the edge O-Mo bonds has a weaker vdW-interlayer interaction as explained by Li *et al.*<sup>8</sup> because of the AB stacking of the puckered honeycomb lattice. Thus, the  $M_s$  value monotonically increases with increasing  $d$  as shown in Fig. 4(b). Moreover, since the oxidation of pore edges is easily obtained only by exposing MoS<sub>2</sub>-NMs to air, all dangling bonds of pore edges in each NM can be fully O-terminated and can easily provide a robust FM even at room temperature. Consequently, the present finding of edge-spin-derived room-temperature FM must enable the use of atomically thin (or few-layer) MoS<sub>2</sub> in unique magnetic and spintronic applications in addition to well-established electronic and photonic applications.

See [supplementary material](#) for methods for sample preparations and calculations.

The authors thank T. Enoki, T. Ando, A. Ishii, G. Fiori, A. H. Macdonald, P. Seneor, R. Wiesendanger, M. Dresselhaus, J. Shi, and P. Kim for their technical contributions, fruitful discussions, and encouragement. The work at the Aoyama Gakuin University was partly supported by a grant for private universities awarded by MEXT. The work at the University of Tokyo was also supported by Grant Nos. 26103003, 25247051, and 15K17676.

<sup>1</sup> J. Haruyama, "Special issue on 'Carbon Nanoelectronics,'" *Electronics* **2**(4), 368–386 (2013).

<sup>2</sup> T. Hashimoto, J. Haruyama, D. Soriano, and S. Roche, *Appl. Phys. Lett.* **105**, 183111 (2014).

<sup>3</sup> Y. Nakanishi, A. Ishi, C. Ohata, D. Soriano, R. Iwaki, K. Nomura, M. Hasegawa, T. Nakamura, S. Katsumoto, and S. Roche, *Nano Research* **10**, 718 (2017).

<sup>4</sup> C. Ohata, R. Tagami, Y. Nakanishi, R. Iwaki, K. Nomura, and J. Haruyama, *Appl. Phys. Lett.* **109**, 133110 (2016).

<sup>5</sup> M. Chowalla, H. S. Shin, G. Eda, L.-J. Li, K. P. Loh, H. Zhang, *Nature Commun.* **5**, 263 (2013).

- <sup>6</sup> Y. Katagiri, T. Nakamura, A. Ishii, C. Ohata, M. Hasegawa, S. Katsumoto, T. Cusati, A. Fortunelli, G. Iannaccone, G. Fiori, S. Roche, and J. Haruyama, "Gate-tunable atomically thin lateral MoS<sub>2</sub> Schottky junction patterned by electron beam," *Nano Letters* **16**, 3788 (2016).
- <sup>7</sup> Y. Katagiri, T. Nakamura, C. Ohata, S. Katsumoto, and J. Haruyama, *Appl. Phys. Lett.* **110**, 143109 (2017).
- <sup>8</sup> Y. Li, Z. Zhou, S. Zhang, and Z. Chen, *J. Ame. Chem. Soc.* **130**, 16739 (2008).
- <sup>9</sup> B. Xia, D. Gao, P. Liu, Y. Liu, S. Shi, and K. Tao, *Physical Chemistry Chemical Physics* **48**, 32505 (2015).
- <sup>10</sup> N. Huo, Y. Li, J. Kang, R. Li, Q. Xia, and J. Li, *Appl. Phys. Lett.* **104**, 202406 (2014).
- <sup>11</sup> Z. Zhang, X. Zou, V. H. Crespi, and B. I. Yakobson, *ACS Nano* **7**, 10475 (2013).
- <sup>12</sup> L. Cai, J. He, Q. Liu, T. Yao, L. Chen, W. Yan, F. Hu, Y. Jiang, Y. Zhao, T. Hu, Z. Sun, and S. Wei, *J. Am. Chem. Soc.* **137**, 2622 (2015).
- <sup>13</sup> G. Gao, C. Chen, X. Xie, Y. Su, S. Kang, G. Zhu, D. Gao, A. Trampert, and L. Cai, *Materials Research Lett.* (2016).
- <sup>14</sup> D. Gao, M. Si, J. Li, J. Zhang, Z. Zhang, Z. Yang, and D. Xue, *Nanoscale Research Lett.* **8**, 129 (2013).
- <sup>15</sup> H. Zhang, X.-B. Li, and L.-M. Liu, *J. Appl. Phys.* **114**, 093710 (2013).
- <sup>16</sup> L. H. Li and Y. Chen, *J. Appl. Phys.* **116**, 213904 (2014).
- <sup>17</sup> S. Mathew *et al.*, *Appl. Phys. Lett.* **101**, 102103 (2012).
- <sup>18</sup> J. Wang *et al.*, *Appl. Phys. Lett.* **109**, 092401 (2016).
- <sup>19</sup> S. Bae *et al.*, *Phys. Rev. Applied.* **7**, 024001 (2017).